BioOne DIGITAL LIBRARY

Dermal Denticle Patterning in the Cretaceous Hybodont Shark Tribodus limae (Euselachii, Hybodontiformes), and Its Implications for the Evolution of Patterning in the Chondrichthyan Dermal Skeleton

Authors: Maisey, John G., and Denton, John S. S.

Source: Journal of Vertebrate Paleontology, 36(5)

Published By: The Society of Vertebrate Paleontology

URL: https://doi.org/10.1080/02724634.2016.1179200

The BioOne Digital Library (https://bioone.org/) provides worldwide distribution for more than 580 journals and eBooks from BioOne's community of over 150 nonprofit societies, research institutions, and university presses in the biological, ecological, and environmental sciences. The BioOne Digital Library encompasses the flagship aggregation BioOne Complete (https://bioone.org/subscribe), the BioOne Complete Archive (https://bioone.org/archive), and the BioOne eBooks program offerings ESA eBook Collection (https://bioone.org/esa-ebooks) and CSIRO Publishing BioSelect Collection (https://bioone.org/csiro-ebooks).

Your use of this PDF, the BioOne Digital Library, and all posted and associated content indicates your acceptance of BioOne's Terms of Use, available at www.bioone.org/terms-of-use.

Usage of BioOne Digital Library content is strictly limited to personal, educational, and non-commmercial use. Commercial inquiries or rights and permissions requests should be directed to the individual publisher as copyright holder.

BioOne is an innovative nonprofit that sees sustainable scholarly publishing as an inherently collaborative enterprise connecting authors, nonprofit publishers, academic institutions, research libraries, and research funders in the common goal of maximizing access to critical research.

Downloaded From: https://complete.bioone.org/journals/Journal-of-Vertebrate-Paleontology on 24 Mar 2025
Terms of Use: https://complete.bioone.org/terms-of-use

Journal of Vertebrate Paleontology e1179200 (10 pages)
Published with license by the Society of Vertebrate Paleontology
DOI: 10.1080/02724634.2016.1179200

ARTICLE

DERMAL DENTICLE PATTERNING IN THE CRETACEOUS HYBODONT SHARK *TRIBODUS LIMAE* (EUSELACHII, HYBODONTIFORMES), AND ITS IMPLICATIONS FOR THE EVOLUTION OF PATTERNING IN THE CHONDRICHTHYAN DERMAL SKELETON

JOHN G. MAISEY* and JOHN S. S. DENTON
Division of Paleontology, American Museum of Natural History, Central Park West at 79th Street, New York, New York 10024-5192, U.S.A, maisey@amnh.org; jdenton@amnh.org

ABSTRACT—As in modern elasmobranchs (sharks and rays), the shagreen of the hybodontiform shark *Tribodus limae* (Santana Formation, Aptian-Albian, Lower Cretaceous, northeastern Brazil) consists of non-growing (monodontode) dermal denticles that were shed, replaced, and supplemented by new ones during life. In modern elasmobranchs, these denticles are usually represented by a single size class (considered here to be the default arrangement), although larger denticles are sometimes present locally (e.g., thorn rows on the head and trunk in batomorphs). In *Tribodus*, however, the shagreen consists of two distinct morphological denticle types and size classes (two-size), both widely distributed over the body and fins, with smaller denticles overlying the bases of larger thorns as well as occupying areas between them. Using two conceptually distinct variants of a two-layer reaction-diffusion (R-D) simulation that is consistent with morphogen exchange across the basal lamina between the epidermal and dermal layers, we recovered two-size spatial arrangements similar to the *Tribodus* shagreen. Our results suggest that denticle patterning in the dermal skeleton of sharks can be replicated using R-D models with kinetics similar to those previously applied to a known mechanism of feather bud patterning in birds and to skin pigmentation patterning in modern teleost fishes. Reaction-diffusion simulations operationalize Reif's 'odontode regulation theory,' and so have an important conceptual place in the history of research on the dermal skeleton. Such a modeling framework may enable conceptual links to be drawn among seemingly disparate denticle arrays in Paleozoic and recent chondrichthyans, thereby guiding future work on the molecular and histological underpinnings of dermal skeleton development and evolution.

Citation for this article: Maisey, J. G., and J. S. S. Denton. 2016. Dermal denticle patterning in the Cretaceous hybodont shark *Tribodus limae* (Euselachii, Hybodontiformes), and its implications for the evolution of patterning in the chondrichthyan dermal skeleton. Journal of Vertebrate Paleontology. DOI: 10.1080/02724634.2016.1179200.

INTRODUCTION

The skin of most elasmobranchs (sharks, rays) is densely covered with a shagreen of small, non-growing dermal denticles (placoid scales), each derived ontogenetically from an individual odontode (i.e., monodontode sensu Ørvig, 1977) and tightly anchored in the mesenchymal stratum compactum by bundles of collagenous Sharpey's fibers (Meyer and Seegers, 2012). It has long been known that denticle formation involves both ectoderm and ectomesenchyme (Hertwig, 1874). Monodontode dermal denticles also occur in modern chimaeroids (although oropharyngeal denticles are absent), but are restricted to certain parts of the body and are better developed in juveniles than in adults (Dean, 1906; Patterson, 1965; Didier, 1995). Although there is strong circumstantial evidence that modern chondrichthyan dermal and oropharyngeal denticles are periodically shed (Peyer, 1968; Reif, 1974), replacement rates are still largely unknown.

Modern elasmobranch denticles are arranged in a single layer, typically with non-overlapping bases (unlike osteichthyan scales, where each scale base overlaps the one behind). Adjacent denticle bases are occasionally fused, although this phenomenon is comparatively rare and never includes the crown (e.g., in *Echinorhinus*; Bigelow and Schroeder, 1948). However, compound scales (polyodontode denticles sensu Ørvig, 1977), consisting of fused and overlapping odontodes of different sizes, are commonly present in Paleozoic chondrichthyans.

Denticle density in modern elasmobranchs is systematically consistent (Reif, 1985b); patterns range from closely packed (e.g., *Orectolobus*) to widely scattered (e.g., *Echinorhinus*), suggesting that spacing of denticles is not random, but highly regulated. Modern elasmobranch dermal denticles may also display regional variation (e.g., enlarged denticles on the upper surface of the pectoral fin, on the head, along the dorsal margin of the caudal fin, and on the ventral surface of the caudal peduncle; Kemp, 1999). Besides providing protection from abrasion, elasmobranch skin denticles may also improve hydrodynamic efficiency, especially in fast-swimming sharks (Reif and Dinkelacker, 1982; Raschi and Musick, 1984; Raschi and Elsom, 1986). Neurosensory pit organs in the skin are often accompanied by specialized accessory denticles (Reif, 1985a), and other specialized denticles border the lateral line in *Chlamydoselachus* (Gudger and Smith, 1933), suggesting that the spatial and morphological patterning of denticles can be modified by proximity to these sensory organs. In the Port Jackson shark *Heterodontus* (a relatively sluggish, bottom-dwelling form), denticle morphology not only varies according to the position on the body, but also with growth (Reif, 1974). Whereas some denticle

*Corresponding author.
© John G. Maisey and John S. S. Denton
This is an Open Access article distributed under the terms of the Creative Commons Attribution-NonCommercial-NoDerivatives License (http://creativecommons.org/licenses/by-nc-nd/4.0/), which permits non-commercial re-use, distribution, and reproduction in any medium, provided the original work is properly cited, and is not altered, transformed, or built upon in any way.

Downloaded From: https://complete.bioone.org/journals/Journal-of-Vertebrate-Paleontology on 24 Mar 2025
Terms of Use: https://complete.bioone.org/terms-of-use

morphologies seem to have a restricted systematic occurrence (e.g., among various carcharhinoid families; Compagno, 1988), other types are more widespread (e.g., the short-crowned, multicusped, and multi-ridged denticles of larger carcharhinoid and lamniform sharks; White, 1937). Morphological differences have been noted between skin denticles and those lining the buccal cavity, gill arches, and pharynx (Imms, 1905), perhaps reflecting their divergent functional specialization (Clark and Nelson, 1997; Atkinson and Collin, 2012).

Elasmobranch denticles do not typically display an ordered arrangement like that of osteichthyan scales, although denticles of the trunk region sometimes assume a diagonal-row-like positioning (e.g., *Carcharhinus, Triaenodon, Prionace, Sphyrna*; Reif, 1985b), reminiscent of some microsquamous extinct fishes (e.g., *Acanthodes, Cheirolepis*; Janvier, 1996). Some recent phylogenies resolve chondrichthyans as nested among 'bony' fishes (Davis et al., 2012; Zhu et al., 2013), raising the possibility that the absence of osteichthyan-like scale organization in chondrichthyans is secondary rather than primitive. Despite the seemingly disorganized distribution of denticles in the skin of most adult elasmobranchs, the ontogenetically earliest denticles may be arranged in distinct rows at specific sites: on either side of the caudal fin axis in *Heterodontus* (Johanson et al., 2007), from the pectoral fins to the caudal peduncle in *Scyliorhinus* (Freitas and Cohn, 2004), and along both sides of the caudal peduncle in *Cephaloscyllium* and *Squalus* (Grover, 1974; Maisey, 1974). Thus, initial denticle patterning in elasmobranchs can be highly organized, but this transient stage can disappear secondarily; in skates, however, some of the first denticles to form in juveniles are arranged in rostrocaudal rows that are retained into adulthood (Grover, 1974; Miyake et al., 1999). It has been suggested that initial denticle patterning in *Heterodontus* is related to myomere pattern (Johanson et al., 2007), as with osteichthyan scales (Sire and Akimento, 2004). In these cases, the higher-order arrangement of denticles may vary according to the underlying structure of earlier-developing chemical gradients.

By contrast, the dermal denticles in *Tribodus* present a novel pattern, in that they appear to be both randomly and evenly distributed, but are of two distinct size classes (described below). This unusual condition reiterates the importance of fossil taxa for presenting mosaic character states either unseen or uncommon in extant forms (Donoghue et al., 1989), and also raises more specific questions about how the developmental underpinnings of such a two-size dermal patterning may relate to the more commonly observed patterns of a single size class in extant taxa.

Although squamation patterns of dermal denticles or pigmentation are often geometrically arranged, they can be difficult to discretize. However, since the mid-20th century, the fit of increasingly elaborate mathematical models of reaction-diffusion (R-D) chemical dynamics (e.g., Turing, 1952; Yang et al., 2002; Barrio et al., 2009; Badugu et al., 2012; Maini et al., 2012; Madzvamuse et al., 2015) to different biological case studies of cutaneous tissues (e.g., Kondo and Asai, 1995; Yamaguchi et al., 2007; Barrio et al., 2009; Kondo and Miura, 2010) suggests that such conceptual models may potentially approximate the actual dynamics of spatial patterning in cutaneous tissues generated by combinations of activator/inhibitor transcription factors (e.g., the WNT/DKK interactions in feather bud spatial patterning; Sick et al., 2006). As applied to dermal denticles, for example, such models are intuitively appealing because they operationalize the inhibitory field and odontode regulation theories of Reif (1980, 1982), who—with remarkable foresight—postulated that denticle development occurred as the outcome of diffusion gradients of an inhibiting signal through the epidermis.

However, unlike pigmentation patterns, which are related to the differential distribution of melanocyte cells, dermal denticles form de novo at the interface of the epidermis and dermis, on the basal lamina (e.g., Miyake et al., 1999; Barrio et al., 2009). Reaction-diffusion models that involve coupling between layers (Yang et al., 2002; Barrio et al., 2009; Madzvamuse et al., 2015) approximate the interaction of morphogens through the basal lamina between the epidermal and dermal layers. Such coupled models can recover patterns of two-size spatial arrangements, regardless of both the kind of interactions taking place across layers and the assumed kinetics of the R-D system (Barrio 2008).

Institutional Abbreviation—AMNH, American Museum of Natural History, New York, U.S.A.

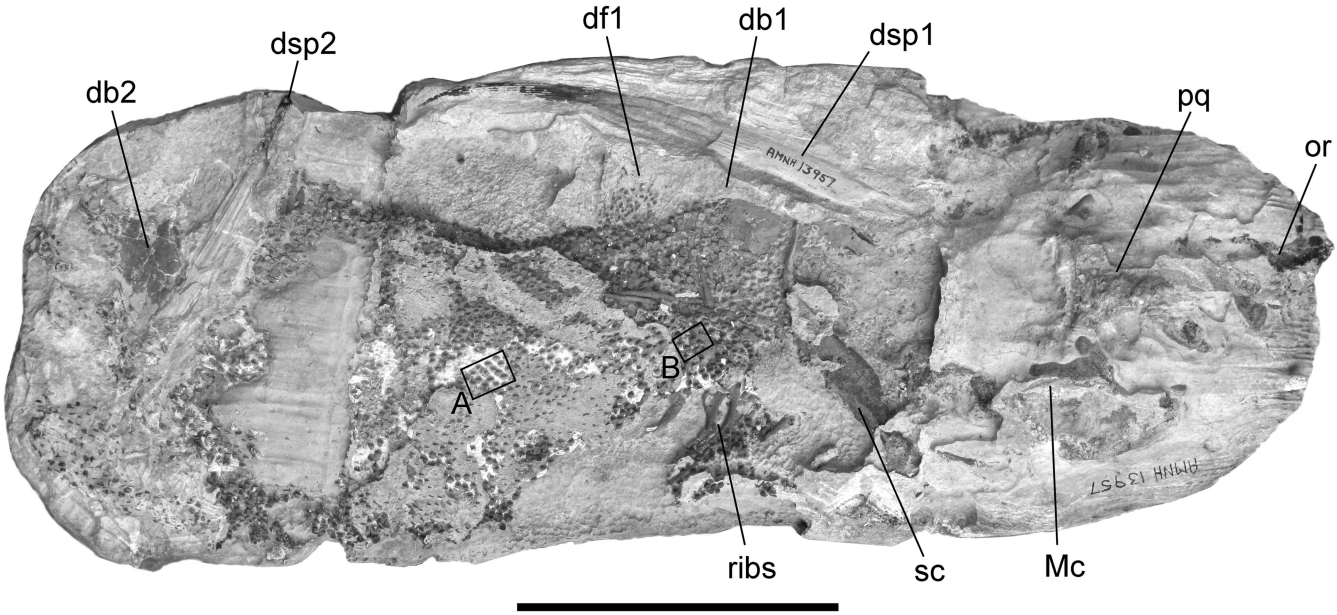

FIGURE 1. *Tribodus limae*, AMNH FF13957, general view of the specimen showing landmark features and regions of shagreen (boxes A and B) shown in Figure 2. **Abbreviations**: **db1**, **db2**, basal cartilage of first and second dorsal fins; **df1**, first dorsal fin; **dsp1**, **dsp2**, first and second dorsal fin spines; **Mc**, Meckel's cartrilage; **or**, orbit; **pq**, palatoquadrate; **sc**, scapulocoracoid. The position of several calcified pleural ribs is also indicated. Scale bar equals 10 cm.

Downloaded From: https://complete.bioone.org/journals/Journal-of-Vertebrate-Paleontology on 24 Mar 2025
Terms of Use: https://complete.bioone.org/terms-of-use

MATERIALS AND METHODS

Imaging of Denticles

Our investigation of denticle morphology in *Tribodus limae* is based primarily on a single specimen, AMNH FF13957, including the head, trunk, fins, and spines of a single individual (Fig. 1). Additional information concerning oropharyngeal denticles in *T. limae* was provided by AMNH FF13959. Both specimens have been illustrated previously (Lane and Maisey, 2009: fig. 1).

Chemical preparation in dilute acetic acid dissolved much of the carbonate matrix covering both specimens, exposing many dermal denticles in situ (Figs. 2, 3) and freeing many more from the matrix; these were investigated by means of scanning electron microscopy (Figs. 4, 5). However, acid preparation was suspended before completion, leaving the majority of denticles in situ and providing a snapshot of their distribution.

Isolated denticles recovered from AMNH FF13957 were mounted and sputter coated with gold palladium for 75 seconds, and then photographed on a Zeiss EVO 60 environmental scanning electron microscope (SEM) at 10 kV with a vacuum of 7.0 × 10e-6 millibars.

Simulation of Denticle Development and Spatial Arrangement Using Coupled R-D Dynamics

Both tooth and denticle development are preceded by a thickening of epidermal tissue, followed by recruitment of

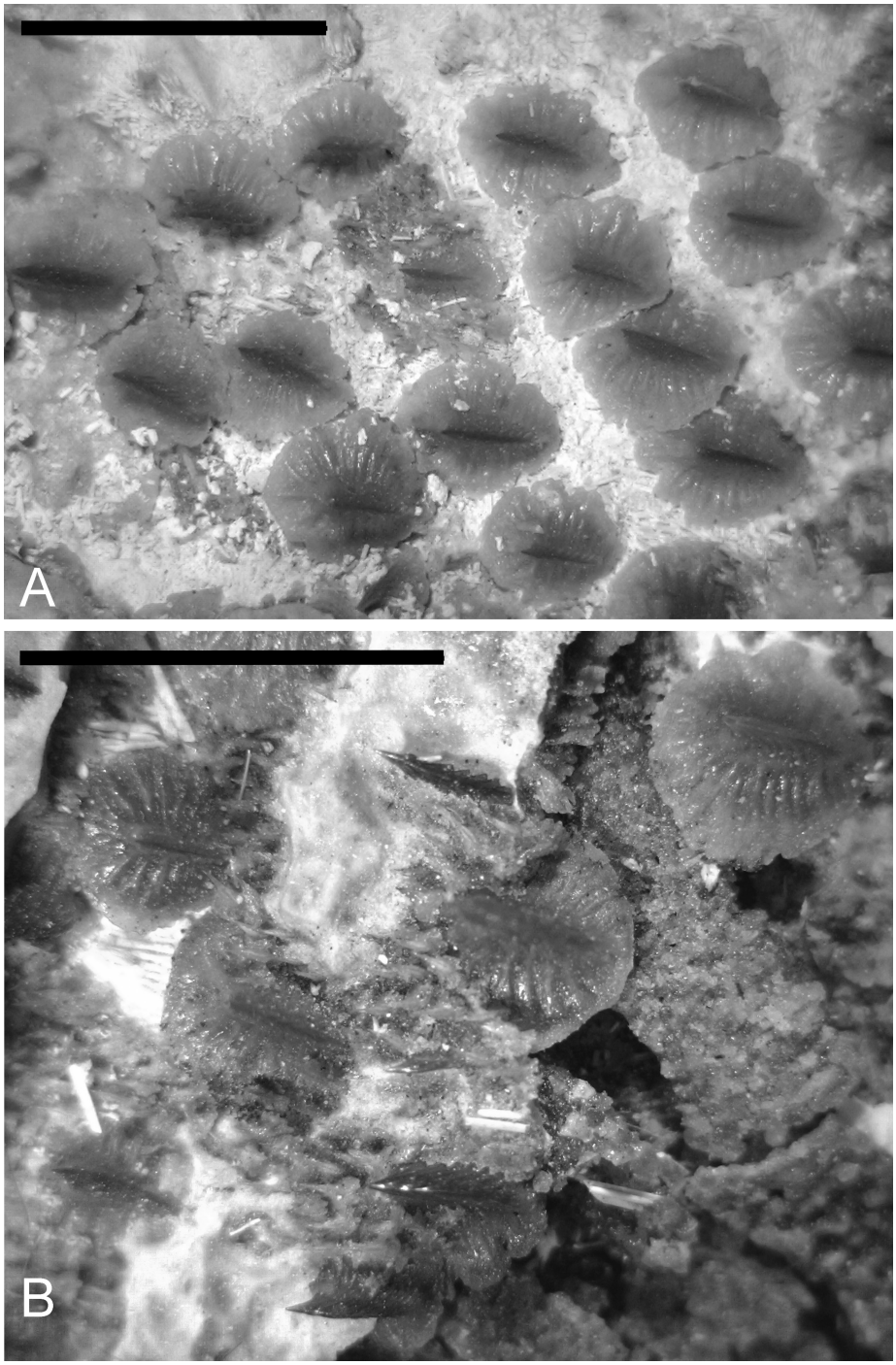

FIGURE 2. Exposed regions of the dermal squamation in AMNH FF13957, corresponding to boxes **A** and **B** in Figure 1. **A**, right side of trunk midway between dorsal fins. **B**, right side of trunk below first dorsal fin. Lower right corner of each box points anteriorly. Large denticles are loosely organized in diagonal rows, some with overlapping bases. Note the numerous very small denticles between larger thorns. White fibrous bundles of phosphatized muscle fibers underlie many of the denticles. Scale bars equal 5 mm.

Downloaded From: https://complete.bioone.org/journals/Journal-of-Vertebrate-Paleontology on 24 Mar 2025
Terms of Use: https://complete.bioone.org/terms-of-use

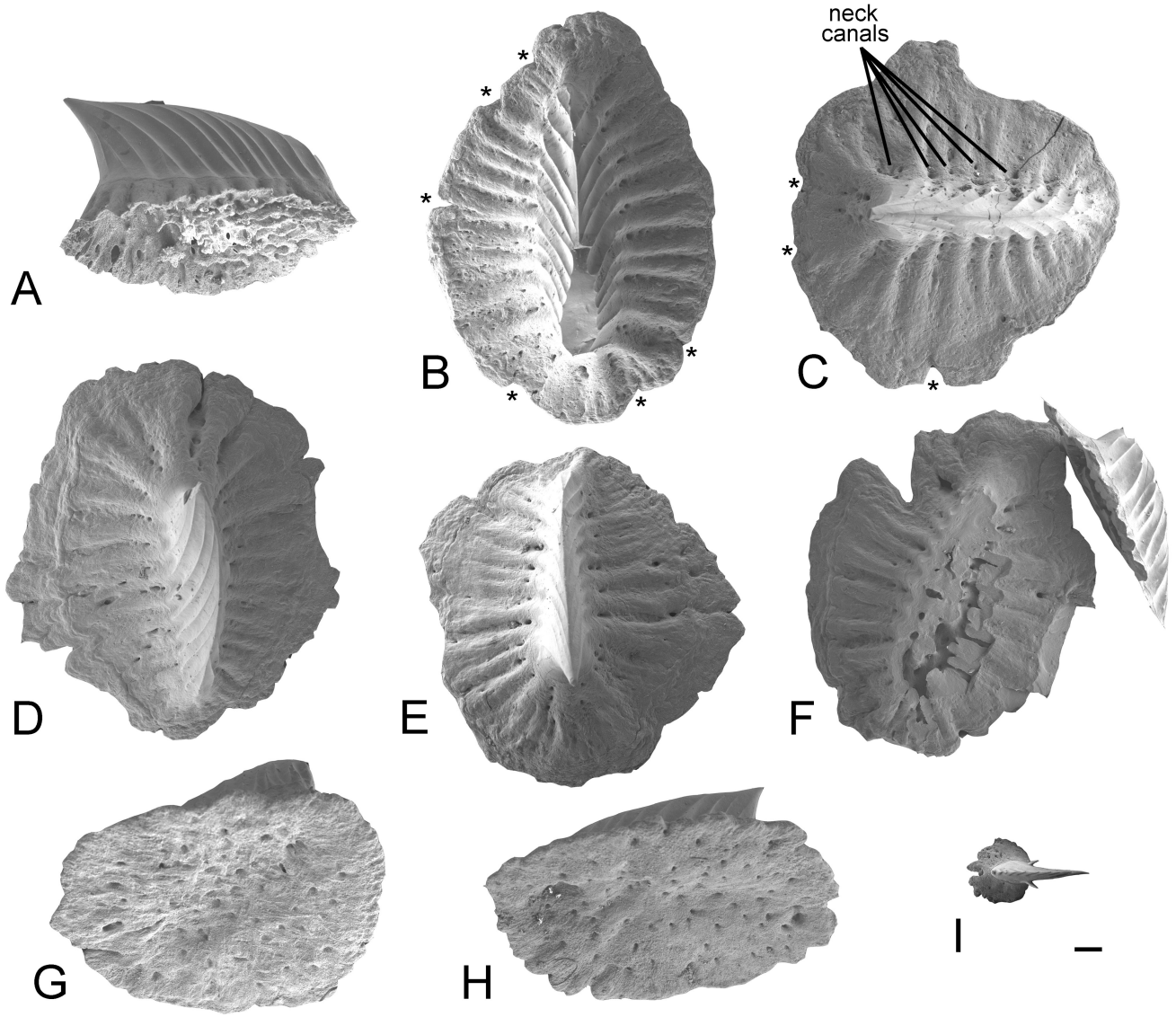

FIGURE 3. SEM images of detached large thorns (**A**–**H**) plus a single small denticle (**I**) from *Tribodus limae* AMNH FF13957. All views are of different denticles harvested from acid preparation residues. The original positions of these denticles on the body are unknown. **A**, presumed newly formed thorn denticle, in which the basal plate has not formed, but there is no pulp cavity; oblique lateral view, left side. **B**–**F**, mature thorn denticles in apical view (the crown has sheared off in **F**, revealing a radial arrangement of vascular canals). **G**, **H**, mature thorn denticles in oblique ventral view, showing the pitted basal plate. **I**, small 'cock's comb' denticle (also shown in **H**) for size comparison. Scale bar equals 100 μm.

mesenchymal cells and subsequent differentiation, and thus involve interaction across tissue layers (Thesleff and Hurmerinta, 1981; Sire et al., 1997; Miyake et al., 1999; Sire and Huysseune, 2003). Although the molecular interactions in tooth development are known for mammal (mouse), bony fish (zebrafish), and chondrichthyan models (Fraser et al., 2010, 2013), and also for teleost scales (Sire and Akimenko, 2004; Fraser et al., 2010), gene interaction networks involved in dermal denticle morphogenesis remain largely unknown, although recent work suggests that bone morphogenetic protein (BMP), fibroblast growth factor (FGF), paired-like homeodomain transcription factor (PITX), sonic hedgehog (SHH), and Msh homeobox (MSX) may contribute significantly (Debiais-Thibaud et al., 2015). Unpublished findings by L. Rasch also implicate wingless-related integration site (WNT) in denticle morphogenesis.

Reaction-diffusion simulation using biological molecular pathways in the kinetic component requires reaction quantification in order to derive the differential equations on which the kinetics are based. Ideally, a model accounting for the kinetics of all morphogens associated with denticle morphogenesis would provide the most predictive power. However, quantified interactions among the major molecular components of denticle morphogenesis have not been presented. Therefore, our investigation simulated the development of two-size dermal denticles on a $256 \times 256 \times 1$ grid, using two linearly coupled models of well-known R-D systems: one with Brusselator kinetics (Yang et al., 2002) and the other with Gierer-Meinhardt (G-M) kinetics modified to parameterize the known reaction dynamics of WNT/DKK interaction in cutaneous feather bud formation (Sick et al., 2006). Brusselator kinetics involve direct chemical interactions among morphogens, whereas G-M kinetics are derived from interaction patterns of biological molecules WNT and DKK, involving non-competitive inhibition at a co-receptor and a saturation term. Both of our simulations used white noise initial

Downloaded From: https://complete.bioone.org/journals/Journal-of-Vertebrate-Paleontology on 24 Mar 2025
Terms of Use: https://complete.bioone.org/terms-of-use

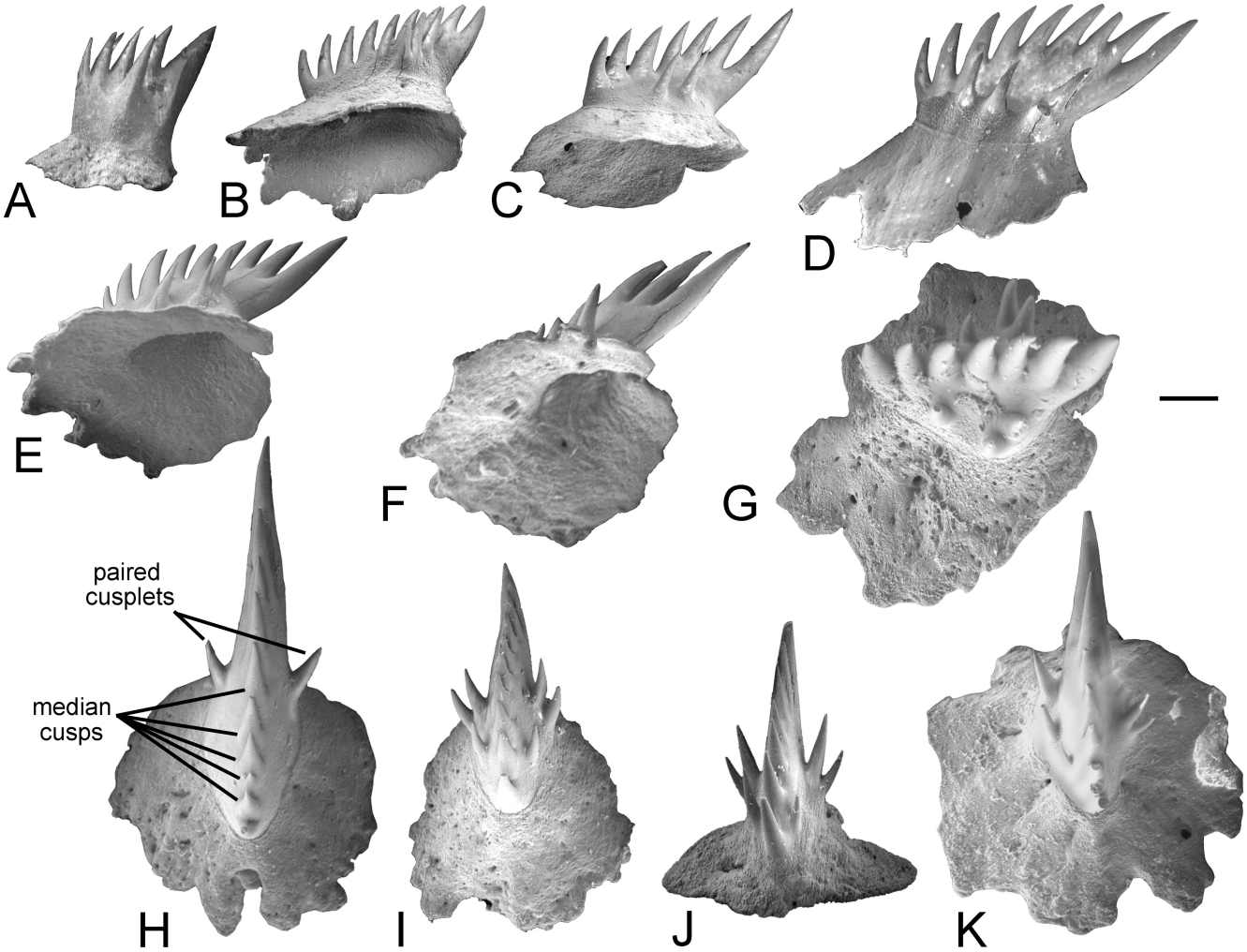

FIGURE 4. SEM images of detached small 'cock's comb' denticles from *Tribodus limae*, AMNH FF13957. **A**–**G**, lateral, ventrolateral, and coronolateral views of several denticles, arranged in order of increasing size; **H**, **I**, **K**, coronal views; **J**, anterior view. Pulp cavity can be seen in **B**, **E**, and **F**. The number of median cusps and paired lateral cusplets is not simply related to denticle size, because even relatively large examples can have fewer cusps and cusplets than smaller ones. The original position of these denticles on the body is unknown, but it is possible that variation in denticle size and in the number and orientation of cusps and paired cusplets are related to the position on the body. Scale bar equals 100 μm.

conditions, assuming equal settings for the two layers (lower = 0.5, upper = 2.0) to parameterize equal initiatory competency. For the Brusselator kinetics, coupling was linear, as in Yang et al. (2002). For G-M kinetics, coupling was quadratic, as in Kyttä (2007). Simulations were conducted in the standalone R-D modeling and visualization program Ready 0.6 (Hutton et al., 2013). A simulation time step (t) of 0.001 was used to improve stability within each iteration, and each simulation was allowed to run to an approximate equilibrium (t >> 150000). Values of the Brusselator kinetic coefficients were set to a = 3, b = 6. Values of the four morphogen diffusion coefficients were constant through time and set to $D_{xi} = 0.5$, $D_{yi} = 9$, $D_{xj} = 12$, and $D_{yj} = 125$. Values of the linear coupling parameters were $\alpha = \beta = 1$. For G-M simulation, values of the reaction kinetic coefficients were set to $\rho_a = 0.05$, $\mu_a = 0.05$, $\rho_b = 0.02$, $\mu_b = 0.015$, $\rho_c = 0.03$, $\mu_c = 0.03$, $\rho_d = 0.015$, $\mu_d = 0.0055$, $\kappa_{ep} = 0.1$, $\kappa_{mes} = 0.005$, $K_{ep} = 0.01$, and $K_{mes} = 0.01$. Values of the four morphogen diffusion coefficients were set to $D_{xi} = 0.005$, $D_{yi} = 0.2$, $D_{xj} = 0.01$, and $D_{yj} = 0.8$. The quadratic coupling parameter, q, was set to -0.0005.

Description of Denticles in *Tribodus limae*

Large thorn-like denticles were first described in *Tribodus limae* by Brito and Ferreira (1989) and subsequently illustrated by Brito (1992:pl. 1, fig. 4a, b). They are non-growing denticles (sensu Reif, 1978), mostly between 2.5 and 4 mm in diameter, with a single blade-like crown and an almost circular base. The distal part of the crown ('thorn') is strongly compressed from side to side, with a convex, blade-like anterior margin (Fig. 3A). The crown expands in width proximally, and its lateral surfaces are ornamented with numerous vertical ridges that rarely bifurcate and become indistinct towards the crown margin. These ridges become wider and farther apart proximally, but do not typically exceed 200 μm in width. The crown is sometimes delimited proximally by a narrow sulcus (Fig. 3B). Accessory cusps have not been found on these denticles.

The denticle base is ovoid in outline and covered by radial ridges that often correspond to vertical ridges on the crown. In fully formed denticles, the base is often scalloped between adjacent ridges. Deeper indentations are sometimes present, possibly

Downloaded From: https://complete.bioone.org/journals/Journal-of-Vertebrate-Paleontology on 24 Mar 2025
Terms of Use: https://complete.bioone.org/terms-of-use

marking the positions of 'soft' structures such as pit organs or slime glands (Fig. 3C, F). Many small pores penetrate the upper surface of the denticle base, especially between the radial ridges. An irregular series of larger pores occurs adjacent to the crown, probably homologous with the neck canals of modern elasmobranch placoid scales (although a neck is absent; Fig. 3). The lower surface of the base is fairly smooth, with numerous scattered pores (Fig. 3G, H). Immature denticles in which the base is not fully formed reveal a spongy trabecular internal structure, lacking a large pulp cavity (Fig. 3A).

Thorn denticles show little sign of wear or abrasion. Adjacent denticles are mostly similar in size, although regional differences are observed (e.g., denticles covering the dorsal fins are slightly smaller than on the adjacent part of the trunk). Most denticle thorns are as tall as long, with a slightly concave posterior margin, but denticles positioned ventrally tend to be shorter, with an almost straight posterior margin. Thorn denticles are distributed fairly uniformly over the body, but some are closer together than others (the maximum distance between them is the equivalent of one scale width). Some denticle bases overlap or even make contact with neighboring ones, but no denticle fusion was observed. A continuous process of denticle formation and loss, replacement, and addition is suggested by the presence of thorn denticles with bases in various states of completeness (e.g., Fig. 3A).

The small denticles in *T. limae* have not previously been reported. Most of these are an order of magnitude smaller than the large ones (ca. 250–600 μm; Fig. 4). They have a very elaborate and ornate crown, with a central crest comprising several acuminate cusps aligned anteroposteriorly like a cock's comb, plus a variable number of acuminate and usually paired accessory cusplets on either side of the central crest. The cusps and cusplets are mostly under 50 μm maximum diameter, and the longest are ca. 200 μm tall. Several small denticles can occupy the space between thorn denticles, and many of them actually overlie the thorn bases (Fig. 2B). When observed in situ, these denticles are invariably oriented with their cusps directed posteriorly, like the large thorn denticles. As with the thorns, the small denticles differ according to their position on the body (e.g., fewer accessory cusplets are present in denticles from the dorsal fins than elsewhere). Small isolated denticles recovered from acid preparation residues revealed greater morphological variation than among those observed in situ, but because their original location is unknown, the significance of this variation is unclear.

In the smallest denticles (ca. 250 μm long), the central crest is poorly developed and has only four or five cusps, all of approximately equal height but becoming gradually wider posteriorly (Fig. 4A). Only one or two accessory cusplets are present per side, but these are almost as tall as the central cusp. In larger denticles (300–600 μm long), the central crest bears up to nine cusps and becomes progressively taller posteriorly, although the free spines forming the crest are all of approximately the same height; increased crest height primarily involves deepening of the fused proximal parts of the crown. Paired accessory cusplets are generally more numerous in larger denticles (up to five per side in some cases), but these are usually much shorter than the central crest. Anterior cusplets are usually more erect, whereas those farther posteriorly are more divergent posterolaterally. There is considerable variation in the position and extent of cusplets on different denticles: they can be arrayed extensively along both sides of the central cusp or restricted to a smaller region (often situated posteriorly), they can be more or less evenly spaced or almost connected proximally, and they can form rectilinear series or small clusters (Fig. 4D). Although the cusplets are generally paired on either side of the central crest, some are slightly offset from their antimere (Fig. 4K). Despite strong variation in cusplet arrangement, the first cusp of the central crest was never observed to be flanked by cusplets, although these are occasionally present between the first and second central cusps.

Below the crest and accessory cusplets, the crown base is sharply delimited (Fig. 4C, G–I, K). Unlike in the thorn denticles, the base is not ornamented by ridges or grooves, but has a smooth surface pierced by a variable number of pores adjacent to the crown and also near the margin of the base. The base has an irregular, thin margin that is often broken in isolated specimens. Again, unlike the thorn denticles, a large, open pulp cavity is usually present. Thus, despite the complex crown morphology of the small denticles, they nevertheless seem to have formed from a single odontode (sensu Reif, 1978; discussed further below).

Besides these two distinct kinds of skin denticles, *T. limae* also possesses distinctive oropharyngeal denticles, similar to those described in other hybodontiform sharks (Reif, 1978). A few oropharyngeal denticles were observed in situ in AMNH FF13957, and several isolated examples were recovered in acid residues from the same specimen (Fig. 5A–C).

The denticles range in diameter from ca. 500 μm to 1–2 mm, and all have a polygonal outline, with a large, low crown

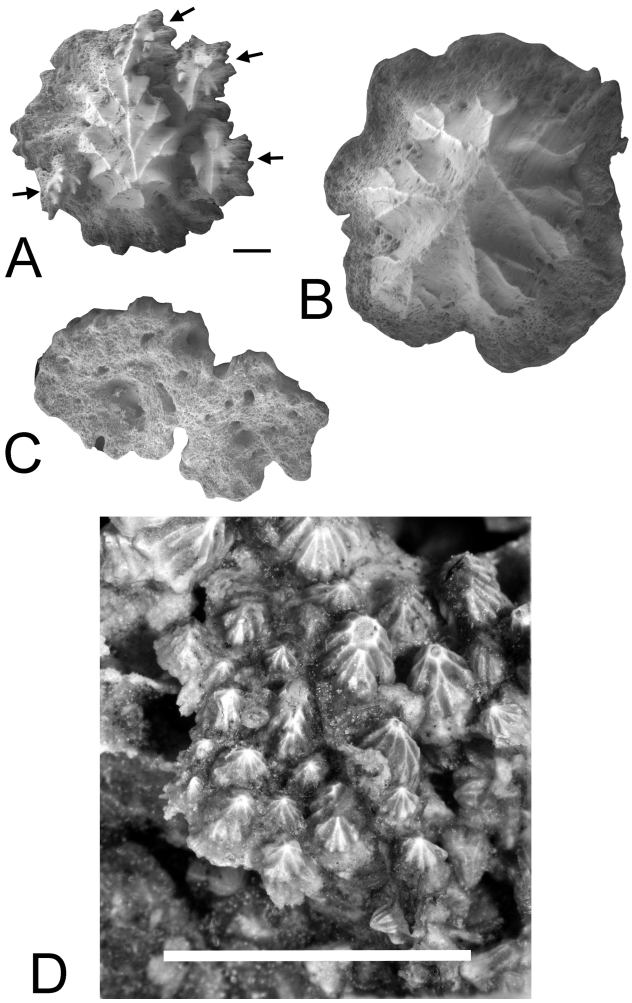

FIGURE 5. Oropharyngeal denticles in *Tribodus limae*. **A**–**C**, individual denticles picked from the oropharynx of AMNH FF13957. **A**, polyodontode denticle with four small denticles accreted to the margins of a larger one, apical view. **B**, single large monodontode denticle, apical view. **C**, two monodontode denticles with fused basal plates, basal view. **D**, monodontode and polyodontode oropharyngeal denticles in situ on branchial cartilages of AMNH FF13959. Scale bars equal 200 μm (**A**–**C**) and 2 mm (**D**).

Downloaded From: https://complete.bioone.org/journals/Journal-of-Vertebrate-Paleontology on 24 Mar 2025
Terms of Use: https://complete.bioone.org/terms-of-use

ornamented with heavy, reticulated ridges covering much of the base. The base is flat and highly vascularized, with numerous pores. Some oropharyngeal denticles have a single crown (Fig. 5B) and can be characterized as non-growing (sensu Reif, 1978), but others are compound scales with several, separate crowns (e.g., Fig. 5A), like the 'growing scales' in *Hybodus delabechei* (Reif, 1978).

Both single-crowned and compound scales of different sizes were observed in situ on the branchial arches in AMNH FF13959, showing that both patterns coexisted simultaneously and in close proximity (Fig. 5D). Thus, *T. limae* seems to have retained evolutionarily primitive compound 'growing' denticles in its oropharyngeal integument, although these are apparently absent from its shagreen.

DISCUSSION

Comparison with Denticles in Other Hybodont Sharks

The survey of denticle morphology in hybodontiform sharks published by Reif (1978) has strongly influenced subsequent phylogenetic and evolutionary consideration of denticle morphology in modern and extinct elasmobranchs (Reif, 1980, 1982; Zangerl, 1981; Maisey, 1982, 1983, 1984a, 1984b, 1986; Maisey et al., 2004). Reif (1978, 1980) found that the integument of some extinct hybodontiform sharks included both 'non-growing' denticles consisting of a single odontode, as well as compound 'growing' denticles with multiple odontodes, each with its own crown, base, and vascular network (e.g., *Hybodus delabechei*), whereas others (e.g., *Egertonodus basanus, E. fraasi, Hybodus obtusus*) apparently had only non-growing denticles, as in modern elasmobranchs. *Tribodus limae* also falls into this category, although its two-size squamation pattern has not yet been observed in other hybodont sharks. Furthermore, the two-size pattern was not seen in the oropharyngeal region of *Tribodus* and appears to be restricted to the external shagreen. This observation suggests that different parameter values and initial conditions may govern denticle growth dynamics in different body regions.

Reif (1978) based much of his characterization of hybodont squamation on dermal denticles recovered from a single acid-prepared specimen of the early Jurassic *Hybodus delabechei*, including both 'non-growing' (monodontode) and 'growing'

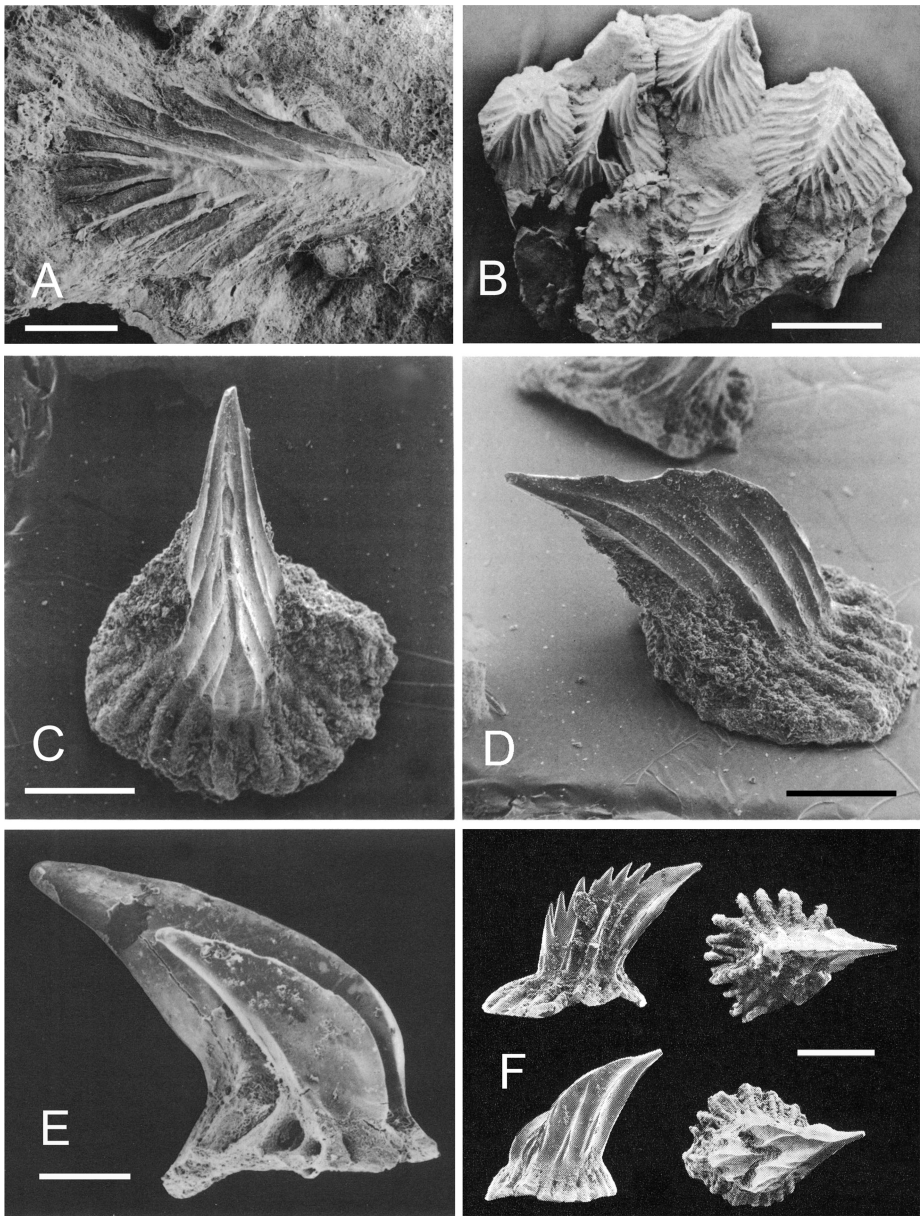

FIGURE 6. Shagreen denticles in other hybodonts. **A**, **B**, denticles from trunk region in *Egertonodus fraasi*, from Maisey (1986). **C, D**, denticles from top of head in *Egertonodus basanus*, from Maisey (1983). **E**, denticles from trunk in *Hamiltonichthys mapesi*, from Maisey (1989). **F**, denticles said to be from near the mouth in *Hybodus delabechei*, after Reif (1978). Scale bars equal 200 μm (**A**, **C**, **D**), 1 mm (**B**), 100 μm (**E**), and 500 μm (**F**).

Downloaded From: https://complete.bioone.org/journals/Journal-of-Vertebrate-Paleontology on 24 Mar 2025
Terms of Use: https://complete.bioone.org/terms-of-use

(polyodontode) types. As he noted, however, the original position of many denticles was uncertain, particularly polyodontode ones harvested near the mouth. This is crucial because, following his study, it has often been assumed that polyodontode and monodontode denticles co-occurred over the body in *H. delabechei*, implying some kind of 'transition' between Paleozoic chondrichthyans (mostly characterized by polyodontode denticles) and the modern monodontode condition. The present observations of denticle morphology in *T. limae* reveal that only its oropharyngeal denticles were polyodontode, whereas its body denticles were monodontode. In fact, Reif's (1978) observations of *H. delabechei* are consistent with ours, because the polyodontode denticles he described and figured from 'near the mouth' are virtually identical to the oropharyngeal denticles in *T. limae*, and may have originated within the oropharynx. Moreover, denticles Reif (1978) recovered from the actual shagreen of *H. delabechei* are morphologically similar to (though much larger than) the small 'cock's comb' denticles found in *T. limae*. Our observations are also in accord with the presence of monodontode shagreen in other Mesozoic and late Paleozoic hybodonts (e.g., *Egertonodus basanus, E. fraasi, Tristychius arcuatus, Hamiltonichthys mapesi*; Brown, 1900; Dick, 1978; Maisey, 1983, 1986, 1989; Fig. 6).

The notion that polyodontode denticles existed outside the oropharyngeal region in hybodonts is therefore questionable, although these denticles were clearly present within the oropharynx of at least some (possibly all) hybodont taxa, unlike in modern elasmobranchs. Instead, the presence of a shagreen consisting entirely of monodontode denticles may be a synapomorphy of hybodonts and modern chondrichthyans, whereas a monodontode oropharyngeal squamation may represent a synapomorphy of the elasmobranch crown group (Maisey 2011, 2012).

Morphogenetic Constraints on Chondrichthyan Dermal Denticle Patterning

In modern elasmobranchs, maintenance of the shagreen during growth involves several morphogenetically coupled factors (Reif, 1974), including denticle coalescence, increased size and/or numbers of replacement denticles, and variable shedding rates. In many extant elasmobranchs, denticles are periodically shed and replaced (Reif, 1974), although replacement rates are still unknown. In certain taxa (e.g., *Isistius, Euprotomicrotus*), the scales do not erupt through the epidermis and are apparently retained for life (Reif, 1980).

Reif (1980) interpreted variation in squamation patterns of extant elasmobranchs (and some extinct chondrichthyans; e.g., *Protacrodus, Ctenacanthus costellatus, Hybodus delabechei*) using morphogenetic parameters that allowed him to conceptualize several morphogenetic 'types' of dermal skeletons and led him to develop his 'inhibitory field theory' (IFT) of denticle formation.

The concept underlying the IFT is similar to R-D systems, in that IFT assumes that diffusion of a morphogenetic field through tissue is responsible for denticle patterning (Donoghue, 2002). However, the IFT assumes that differential inhibition alone is sufficient for generating complex spatial patterning. Inhibitory field theory may therefore be seen as a verbal hypothesis of a restricted parameterization of R-D systems, consisting of a single inhibitory component, and no kinetic component. Such a system is by itself insufficient for generating the two-size condition observed in *Tribodus*.

Although R-D models in their traditional formulations can inform only on the spatial arrangement of denticle placement, and not about the development of the denticle morphology itself, our coupled R-D simulation nevertheless recovered a very close approximation of the *Tribodus* shagreen (Fig. 7A–C), regardless of the assumed kinetic model, consisting of a randomly distributed, evenly spaced two-size pattern with ~4:1 large:small size ratios of the element diameters and spacing of five to six small denticles between large ones. This result is consistent with the success of previous R-D simulation studies in recovering complex cutaneous patterns (e.g., Barrio et al., 2009; Kondo and Miura, 2010). The G-M model (Fig. 7C) differed from the Brusselator model (Fig. 7B) in generating a patchier distribution of the two size classes, a result that may or may not be more congruent with the observed distribution in *Tribodus*, depending on considerations of possible taphonomic deformation, débridement, and incomplete preparation.

This study is the first application of R-D dynamics to the problem of dermal denticle patterning, and we also believe it to be the first to apply R-D formulations in paleontology. We feel that approaches like this are beneficial for augmenting the axes of inclusion between neontological and paleontological questions. For example, the flexibility of R-D modeling may provide a future framework for approaching complex questions in the evolution of spatial arrangements, such as heterotopy (Zelditch and Fink, 1996). Although the

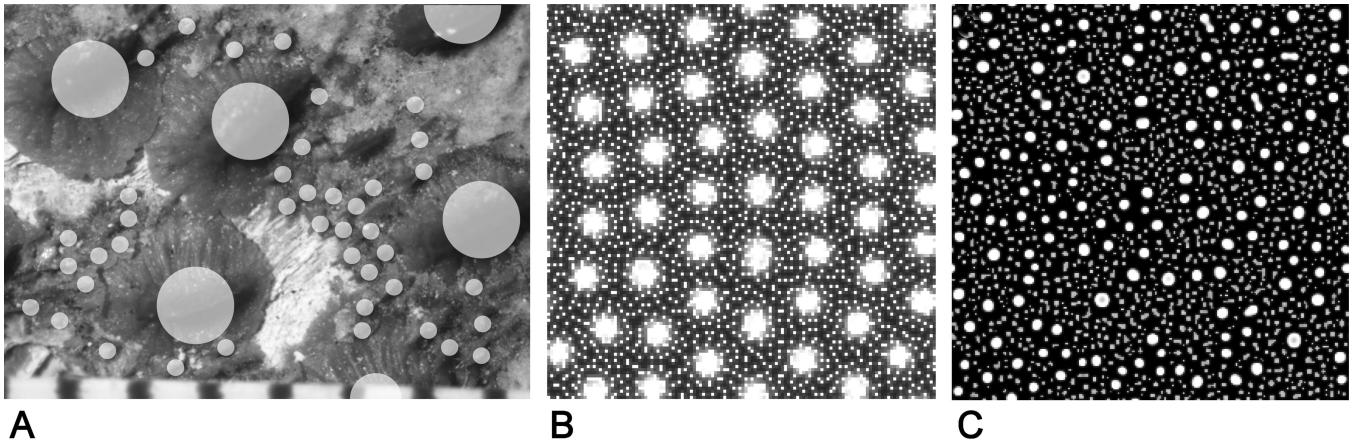

FIGURE 7. Approximation of the dermal shagreen of *Tribodus limae* patterning through simulation of a coupled reaction-diffusion (R-D) system with both Brusselator and Gierer-Meinhardti (G-M) kinetics. **A**, dermal denticles of *Tribodus limae*, AMNH FF13959, with crown areas highlighted to distinguish positional spacing from individual denticle morphology. **B**, Brusselator R-D equilibrium patterns of one activator morphogen, with model coefficients defined in text, showing distributional differences in activator expression level (black equals 0, white equals 5; arbitrary units). **C**, G-M R-D equilibrium pattern of one activator morphogen, with model coefficients defined in text, showing differences from Brusselator kinetics and distributional differences in both clustering of two size classes and in activator expression level (black equals 0, white equals 5; arbitrary units).

Downloaded From: https://complete.bioone.org/journals/Journal-of-Vertebrate-Paleontology on 24 Mar 2025
Terms of Use: https://complete.bioone.org/terms-of-use

Tribodus two-size pattern appeared to be restricted to the dermal shagreen and was not observed in the oropharyngeal region, the two different body regions may share a common coupled R-D system differing only in initial conditions (e.g., Bard and Lauder, 1974). Coupled R-D systems may therefore be a general foundation from which the dermal skeleton is derived, but we suggest such hypotheses and apply such simulations cautiously. Denticle patterning is a different class of problem than pigmentation, in terms of the elements being arranged (pigment cells versus calcification sites), and the absence of known reaction kinetics limits the degree to which predictions can be made about denticle growth. However, the largely congruent fit of R-D modeling using both chemically and biologically informed kinetic pathways at different ends of the conceptual spectrum of how one approaches parameterization (Rice, 2004) suggests that the observed pattern may, with careful consideration, be robust to the assumed underlying mechanism. Such a result opens up the possibility that seemingly disparate denticle arrays seen in both ancient and modern chondrichthyans may be connected through changes in parameter values within simple models of R-D mechanics, an idea recently intimated for transformations among Turing nanopatterns in insect corneae (Fig. 4; Blagodatski et al., 2015).

ACKNOWLEDGMENTS

This research was supported by the Herbert and Evelyn Axelrod Research Chair in Paleoichthyology at the AMNH. We thank G. Naylor for introducing J.S.S.D. to the subject of pattern modeling, and T. Hutton for discussion on the functionality of Ready 0.6.

LITERATURE CITED

Atkinson, C. J. L., and S. P. Collin. 2012. Structure and topographic distribution of oral denticles in elasmobranch fishes. Biology Bulletin 222:26–34.

Badugu, A., C. Kraemer, P. Germann, D. Menshykau, and D. Iber. 2012. Digit patterning during limb development as a result of the BMP-receptor interaction. Scientific Reports 2:991. doi: 10.1038/srep00991.

Bard, J., and I. Lauder. 1974. How well does Turing's theory of morphogenesis work? Journal of Theoretical Biology 45:501–531.

Barrio, R. A. 2008. Turing systems: a general model for complex patterns in nature; pp. 267–296 in I. Licata and A. Sakaji (eds.), Physics of Emergence and Organization. World Scientific Publishing, Hackensack, New Jersey.

Barrio, R. A., R. E. Baker, B. Vaughan Jr., K. Tribuzy, M. R. de Carvalho, R. Bassanezi, and P. K. Maini. 2009. Modeling the skin pattern of fishes. Physical Review E 79:031908.

Bigelow, H. B., and W. C. Schroeder. 1948. Sharks; pp. 59–576, in J. Tee-Van, C. M. Breder, S. H. Hildebrand, A. E. Parr, and W. C. Schroeder (eds.), Fishes of the Western North Atlantic. Memoir of the Sears Foundation for Marine Research, No. 1, Part 1. Yale University, New Haven, Connecticut.

Blagodatski, A., A. Sergeev, M. Kryuchkov, Y. Lopatina, and V. L. Katanaev. 2015. Diverse set of Turing nanopatterns coat corneae across insect lineages. Proceedings of the National Academy of Sciences of the United States of America 112:10750–10755.

Brito, P. M. 1992. Nouvelles données sur l'anatomie et la position systématique de *Tribodus limae* Brito and Ferreira, 1989 (Chondrichthyes, Elasmobranchii) du Crétacé Inférieur de la Chapada do Araripe (N-E Bresil). Geobios 1992:143–150.

Brito, P. M., and P. L. N. Ferreira. 1989. The first hybodont shark, *Tribodus limae* n.g., n.sp., from the Lower Cretaceous of Chapada do Araripe (North-East Brazil). Anais da Academia Brasileira de Ciéncias 61:53–57.

Brown, C. 1900. Über das Genus *Hybodus* und seine systematische Stellung. Palaeontographica 46:149–174.

Clark, E., and D. R. Nelson. 1997. Young whale sharks, *Rhincodon typus*, feeding on a copepod bloom near La Paz, Mexico. Environmental Biology of Fishes 50:63–73.

Compagno, L. J. V. 1988. Sharks of the Order Carcharhiniformes. Princeton University Press, Princeton, New Jersey.

Davis, S, J. Finarelli, and M. I. Coates. 2012. *Acanthodes* and shark-like conditions in the last common ancestor of modern gnathostomes. Nature 486:247–250.

Dean, B. 1906. Chimaeroid Fishes and Their Development. Carnegie Institution of Washington, Washington, D.C., Publication 32, 156 pp.

Debiais-Thibaud, M., R. Chiori, S. Enault, S. Oulion, I. Germon, C. Martinand-Mari, D. Casane, and V. Borday-Birraux. 2015. Tooth and scale morphogenesis in shark: an alternative process to the mammalian enamel knot system. BMC Evolutionary Biology 15:292.

Dick, J. R. F. 1978. On the Carboniferous shark *Tristychius arcuatus* Agassiz from Scotland. Transactions of the Royal Society of Edinburgh 70:63–109.

Didier, D. A. 1995. Phylogenetic systematics of extant chimaeroid fishes (Holocephali, Chimaeroidei). American Museum Novitates 3119: 1–86.

Donoghue, M. J., J. A. Doyle, J. Gauthier, A. G. Kluge, and T. Rowe. 1989. The importance of fossils in phylogeny reconstruction. Annual Review of Ecology and Systematics 20:431–460.

Donoghue, P. C. 2002. Evolution of development of the vertebrate dermal and oral skeletons: unraveling concepts, regulatory theories, and homologies. Paleobiology 28:474–507.

Fraser, G. J., R. F. Bloomquist, and J. T. Streelman. 2013. Common developmental pathways link tooth shape to regeneration. Developmental Biology 377:399–414.

Fraser, G. J., R. Cerny, V. Soukup, M. Bronner-Fraser, and J. T. Streelman. 2010. The odontode explosion: the origin of tooth-like structures in vertebrates. Bioessays 32:808–817.

Freitas, R., and Cohn, M. J. 2004. Analysis of EphA4 in the lesser spotted catfish identifies a primitive gnathostome expression pattern and reveals co-option during evolution of shark-specific morphology. Development Genes and Evolution 214:466–472.

Grover, C. A. 1974. Juvenile denticles of the swell shark *Cephaloscyllium ventriosum*: function in hatching. Canadian Journal of Zoology 52:359–363.

Gudger, E. W., and B. G. Smith. 1933. The natural history of the frilled shark *Chlamydoselachus anguineus*; pp. 245–319 in E. W. Gudger (ed.), Bashford Dean Memorial Volume on Archaic Fishes. American Museum of Natural History, New York.

Hertwig, O. 1874. Ueber Bau und Entwickelung der Placoidschuppen und der Zähne der Selachier. Jenaische Zeitschrift für Naturwissenschaft 8:221–404.

Hutton, T., R. Munafo, A. Trevorrow, T. Rokicki, and D. Wills. 2013. Ready, A Cross-Platform Implementation of Various Reaction-Diffusion Systems, version 0.6. Available at github.com/GollyGang/ready. Accessed April 1, 2014.

Johanson, Z., Smith, M. S., and Joss, J. M. P. 2007. Early scale development in *Heterodontus* (Heterodontiformes; Chondrichthyes): a novel chondrichthyan scale pattern. Acta Zoologica, Stockholm 88:249–256.

Janvier, P. 1996. Early Vertebrates. Oxford Monographs on Geology and Geophysics, Volume 33. Clarendon Press, Oxford, U.K.

Kemp, N. E. 1999. Integumentary system and teeth; pp. 43–68 in W. C. Hamlett (ed.), Sharks, Skates and Rays. John Hopkins University Press, Baltimore, Maryland.

Kondo, S., and R. Asai. 1995. A reaction-diffusion wave on the skin of the marine angelfish *Pomacanthus*. Nature 376:765–768.

Kondo, S., and T. Miura. 2010. Reaction-diffusion model as a framework for understanding biological pattern formation. Science 329:1616–1620.

Kyttä, K. 2007. Computational studies of pattern formation in multiple layer Turing systems; p. 87 in Department of Electrical and Communications Engineering, Vol. M.Sc. Helsinki University of Technology, Helsinki, Finland.

Lane, J. A., and J. G. Maisey. 2009. Pectoral anatomy of *Tribodus limae* (Elasmobranchii: Hybodontiformes), from the Lower Cretaceous of northeastern Brazil. Journal of Vertebrate Paleontology 29:25–38.

Madzvamuse, A., A. H. Chung, and C. Venkataraman. 2015. Stability analysis and simulations of coupled bulk-surface reaction–diffusion

Downloaded From: https://complete.bioone.org/journals/Journal-of-Vertebrate-Paleontology on 24 Mar 2025
Terms of Use: https://complete.bioone.org/terms-of-use

systems. Proceedings of the Royal Society of London A Mathematical, Physical and Engineering Sciences 471. doi: 10.1098/rspa.2014.0546.

Maini, P. K., T. E. Woolley, R. E. Baker, E. A. Gaffney, and S. S. Lee. 2012. Turing's model for biological pattern formation and the robustness problem. Interface Focus rsfs20110113.

Maisey, J. G. 1974. Chondrichthyan dorsal spines and the relationships of spinate chondrichthyans. Ph.D. dissertation, University of London, London, U.K., 592 pp.

Maisey, J. G. 1982. The anatomy and interrelationships of Mesozoic hybodont sharks. American Museum Novitates 2724:1–48.

Maisey, J. G. 1983. Cranial anatomy of *Hybodus basanus* Egerton from the Lower Cretaceous of England. American Museum Novitates 2758:1–64.

Maisey, J. G. 1984a. Chondrichthyan phylogeny: a look at the evidence. Journal of Vertebrate Paleontology 4:359–371.

Maisey, J. G. 1984b. Higher elasmobranch phylogeny and biostratigraphy. Zoological Journal of the Linnaean Society 82:33–54.

Maisey, J. G. 1986. Heads and tails: a chordate phylogeny. Cladistics 2:201–256.

Maisey, J. G. 1989. *Hamiltonichthys mapesi*, g. and sp. nov. (Chondrichthyes; Elasmobranchii), from the Upper Pennsylvanian of Kansas. American Museum Novitates 2931:1–42.

Maisey, J. G. 2011. The braincase of the Middle Triassic shark *Acronemus tuberculatus* (Bassani 1886). Palaeontology 54:417–428.

Maisey, J. G. 2012. What is an 'elasmobranch'? The impact of palaeontology in understanding elasmobranch phylogeny and evolution. Journal of Fish Biology 80:918–951.

Maisey, J. G., G. J. P Naylor, and D. J. Ward. 2004. Mesozoic elasmobranchs, neoselachian phylogeny and the rise of modern elasmobranch diversity; pp. 17–56 in G. Arratia and A. Tintori (eds.), Mesozoic Fishes 3: Systematics, Environments and Biodiversity. Verlag Pfeil, Munich, Germany.

Meyer, W., and U. Seegers. 2012. Basics of skin structure and function in elasmobranchs: a review. Journal of Fish Biology 80:1940–1967.

Miyake, T., J. L. Vaglia, L. H. Taylor, and B. K. Hall. 1999. Development of dermal denticles in skates (Chondrichthyes, Batoidea): patterning and cellular differentiation. Journal of Morphology 241:61–81.

Ørvig, T. 1977. A survey of odontodes ("dermal teeth") from developmental, structural, functional and phyletic points of view; pp. 53–75 in S. M. Andrews, R. S. Miles, and A. D. Walker (eds.), Problems in Vertebrate Evolution. Linnean Society, London, U.K.

Patterson, C. 1965. Phylogeny of the chimaeroids. Philosophical Transactions of the Royal Society of London B 249:101–219.

Peyer, B. 1968. Comparative Odontology. Chicago University Press, Chicago, Illinois, 347 pp.

Raschi, W. G., and J. Elsom. 1986. Comments on the structure and development of the Drag Reduction-Type Placoid scale; pp. 392–407 in T. Uyeno, R. Arai, T. Taniuchi, and K. Matsuura (eds.), Proceedings of the Second International Conference on Indo-Pacific fishes. Ichthyological Society of Japan, Tokyo.

Raschi, W. G., and J. A. Musick. 1984. Hydrodynamic Aspects of Shark Scales. Virginia Institute of Marine Science Special Report in Applied Marine Science and Ocean Engineering No. 272. Virginia Institute of Marine Science, Gloucester Point, Virginia.

Reif, W. E. 1974. Morphologie und Musterbildung im Hautzähnchen-Skelett von *Heterodontus*. Lethaia 7:25–42.

Reif, W. E. 1978. Types of morphogenesis of the dermal skeleton in fossil sharks. Paläontologische Zeitschrift 52:110–128.

Reif, W. E. 1980. A model of morphogenetic processes in the dermal skeleton of elasmobranchs. Neues Jahrbuch für Geologie und Paläontologie, Abhandlungen 159:339–359.

Reif, W. E. 1982. Morphogenesis and function of the squamation in sharks. Neues Jahrbuch für Geologie und Paläontologie, Abhandlungen 164:172–183.

Reif, W. E. 1985a. Functions of scales and photophores in mesopelagic luminescent sharks. Acta Zoologica, Stockholm 66:111–118.

Reif, W. E. 1985b. Squamation and ecology of sharks. Senckenbergische Naturforschende Gesellschaft, Stuttgart 8:1–255.

Reif, W. E., and A. Dinkelacker. 1982. Hydrodynamics of the squamation in fast swimming sharks. Neues Jahrbuch für Geologie und Paläontologie, Abhandlungen 164:184–187.

Rice, S. H. 2004. Evolutionary Theory. Sinauer Associates, Sunderland, Massachusetts.

Sick, S., S. Reinker, J. Timmer, and T. Schlake. 2006. WNT and DKK determine hair follicle spacing through a reaction-diffusion mechanism. Science 314:1447–1450.

Sire, J.-Y., and M. A. Akimento. 2004. Scale development in fish: a review, with description of sonic hedgehog (*shh*) expression in the zebrafish (*Danio rerio*). International Journal of Developmental Biology 48:233–247.

Sire, J.-Y., and A. Huysseune. 2003. Formation of dermal skeletal and dental tissues in fish: a comparative and evolutionary approach. Biological Reviews 78:219–249.

Sire, J.-Y., F. Allizard, O. Babiar, J. Bourguignon, and A. Quilhac. 1997. Scale development in zebrafish (*Danio rerio*). Journal of Anatomy 190:545–561.

Thesleff, I., and K. Hurmerinta. 1981. Tissue interactions in tooth development. Differentiation 18:75–88.

Turing, A. M. 1952. The chemical basis of morphogenesis. Philosophical Transactions of the Royal Society of London B 237:37–72.

White, E. G. 1937. Interrelationships of the elasmobranchs with a key to the Order Galea. Bulletin of the American Museum of Natural History 74(2):25–138.

Yamaguchi, M., E. Yoshimoto, and S. Kondo. 2007. Pattern regulation in the stripe of zebrafish suggests an underlying dynamic and autonomous mechanism. Proceedings of the National Academy of Sciences of the United States of America 104:4790–4793.

Yang, L., M. Dolnik, A. M. Zhabotinsky, and I. R. Epstein. 2002. Spatial resonances and superposition patterns in a reaction-diffusion model with interacting Turing modes. Physical Review Letters 88:208303.

Zangerl, R. 1981. Chondrichthyes I: Paleozoic Elasmobranchii; in O. Kuhn (ed.), Handbook of Paleoichthyology. Gustav Fischer Verlag, Stuttgart, Germany, 115 pp.

Zhu, M., X. Yu, P. E. Ahlberg, B. Choo, J. Lu, T. Qiao, Q. Qu, W. Zhao, L. Jia, H. Blom, and Y. Zhu. 2013. A Silurian placoderm with osteichthyan-like marginal jaw bones. Nature 502:188–193.

Zelditch, M. L., and W. L. Fink. 1996. Heterochrony and heterotopy: stability and innovation in the evolution of form. Paleobiology 22:241–254.

Submitted July 7, 2015; revisions received February 25, 2016;
accepted March 3, 2016.
Handling editor: Martin Brazeau.

Downloaded From: https://complete.bioone.org/journals/Journal-of-Vertebrate-Paleontology on 24 Mar 2025
Terms of Use: https://complete.bioone.org/terms-of-use